# RAGE–TXNIP axis is required for S100B-promoted Schwann cell migration, fibronectin expression and cytokine secretion

**Oualid Sbai[1,*], Takhellambam S. Devi[2,*], Mariarosa A. B. Melone[3], Francois Feron[1], Michel Khrestchatisky[1], Lalit P. Singh[2,4] and Lorena Perrone[1,2,‡]**

[1]NICN, CNRS UMR 6184, Faculté de Médecine, Université Aix-Marseille, 13344 Marseille Cedex 15, France
[2]Department of Anatomy/Cell Biology, Wayne State University School of Medicine, Detroit, MI 48201, USA
[3]Department of Neurological Sciences, Second University of Naples, Naples, 80100, Italy
[4]Department of Ophthalmology, Wayne State University School of Medicine, Detroit, MI 48201, USA
*These authors contributed equally to this work
‡Author for correspondence perrone@ipbs.fr)

*Accepted 27 August 2010*
*Journal of Cell Science 123, 4332-4339*

*doi:10.1242/jcs.074674*

## Summary

During peripheral nerve injury, Schwann cells (SCs) adopt a migratory phenotype and remodel the extracellular matrix and provide a supportive activity for neuron regeneration. SCs synthesize neurotrophic factors and cytokines that are crucial for the repair of the injured nerve. The receptor for advanced glycation end products (RAGE) and its ligand S100B, which are secreted by SCs, are required for the repair of the injured peripheral nerve in vivo. However, the precise intracellular pathways involved have not been completely elucidated. Here, we show that RAGE-induced S100B secretion involves the recruitment of S100B in lipid rafts and caveolae. Moreover, we demonstrate for the first time that RAGE induces the expression of thioredoxin interacting protein (TXNIP) in SCs and the injured sciatic nerve in vivo. TXNIP is involved in the activation of p38 MAPK, CREB and NFκB in SCs. TXNIP silencing partially inhibits RAGE-induced SC migration and completely abolishes RAGE-induced fibronectin and IL-1β expression. Our results support a model in which TXNIP mediates in part RAGE-induced SC migration and is required for the expression of provisional ECM and pro-inflammatory IL-1β. We provide new insight on the role of the SC RAGE–TXNIP axis in the repair of injured peripheral nerves.

**Key words:** S100B, RAGE, TXNIP, Schwann, Migration, Fibronectin, IL-1β

## Introduction

Peripheral nerve injury leads to a program of events that orchestrate a limited inflammatory response due to axonal degeneration and initiates neurite outgrowth; these co-ordinated events are referred to as Wallerian degeneration, in which Schwann cells (SCs) have an essential role (Cheng and Zochodne, 2002). The regeneration capability results from the intrinsic neuronal activities and the activity of surrounding SCs that provide a supportive activity for neuron regeneration (Cheng and Zochodne, 2002). SCs undergo profound phenotypic modification, proliferate and migrate into the distal end in the injured nerve area and synthesize neurotrophic factors and cytokines that are crucial for the repair of the injured nerve (Lisak et al., 1997; Shamash et al., 2002). Despite the numerous studies, the network of molecular events involved is still not completely defined.

The receptor for advanced glycation end products (RAGE) is a multiligand transmembrane receptor that might have either a pathogenic or a beneficial function depending on the cell type (Bierhaus et al., 2005; Rong et al., 2004a; Rong et al., 2004b). RAGE is necessary for the repair of the injured peripheral nerve in vivo (Rong et al., 2004a; Rong et al., 2004b). Injection of the soluble form of RAGE, as well as of blocking antibodies against RAGE or its ligand S100B, suppresses peripheral nerve regeneration, reduces the functional recovery of the nerve and decreases the number of infiltrating phagocytes (Rong et al., 2004a). However, the precise intracellular pathways involved have not been completely elucidated. We have demonstrated that RAGE promotes S100B secretion from SC by recruiting S100B in secretory vesicles and that RAGE triggering induces the phosphorylation of caveolin 1 (cav-1), which is necessary for RAGE-promoted S100B secretion and morphological changes in SCs (Perrone et al., 2008). It has been suggested that cav-1 has a function in myelinating SCs (Mikol et al., 2002) and diabetic neuropathy is exacerbated in *Cav1*$^{-/-}$ mice (Donato et al., 2009). Cav-1 is associated with membrane microdomains that are enriched in cholesterol and sphingolipids and defined as lipid rafts (Cohen et al., 2004; Perrone and Zurzolo, 2003). Here we show that S100B is secreted in cav-1-positive vesicles and that RAGE is internalized in lipid rafts.

During peripheral nerve injury, SCs adopt a migratory phenotype and remodel the extracellular matrix (ECM) so that it is permissive for axonal re-growth (Cheng and Zochodne, 2002). SC migration occurs over the provisional ECM that is produced in part by SCs (Akassoglou et al., 2002; Chernousov and Carey, 2000; Milner et al., 1997). It is still unknown whether RAGE in SCs is implicated in the limited pro-inflammatory response implicated in the nerve repair, as well as in promoting the expression of fibronectin (FN) and SC migration. Engagement of RAGE by S100B leads to a variety of outcomes, from deleterious to beneficial, which are dependent on S100B concentration and the cell type (Donato et al., 2009). We previously reported that the interaction of S100B with RAGE promotes pro-inflammatory gene expression in retinal endothelial cells (ECs) by activating

the expression of thioredoxin-interacting protein (TXNIP) (Perrone et al., 2009). TXNIP is induced by various stresses, interacts with thioredoxin (Trx) and inhibits the antioxidant function of Trx (Kim et al., 2007). TXNIP has diverse functions depending on the cell type, it can regulate cell proliferation, maintain cellular homeostasis, promote IL-1β secretion in macrophages (Zhou et al., 2010), and is also necessary for the development and function of natural killer cells and B lymphocytes (Kim et al., 2007; Shao et al., 2010). We also showed that enhanced TXNIP expression correlates with increased ECM production in mesangial cells (Cheng et al., 2006). However, it is still unexplored whether TXNIP is induced by S100B and whether it mediates RAGE function in SCs. Therefore, we investigated whether the RAGE–TXNIP axis participates in promoting SC migration or limits pro-inflammatory and ECM gene expression following S100B stimulation. We show that RAGE enhances TXNIP expression in primary culture of SCs, and that TXNIP expression is induced during peripheral nerve injury in vivo. TXNIP is required for RAGE-induced p38 MAPK activation. Silencing of TXNIP partially affects S100B-induced SC migration and blocks IL-1β and FN expression. We provide new insight on the role of RAGE–TXNIP axis in SCs, which suggests that this pathway is involved in the repair of the injured peripheral nerve.

## Results

### RAGE induces TXNIP expression in SCs

We demonstrated that in retinal ECs, RAGE stimulation with S100B promotes TXNIP expression, which is required for RAGE-induced gene expression (Perrone et al., 2009). We first analyzed whether RAGE stimulation with S100B induces *Txnip* mRNA expression by quantitative real-time PCR (qRT-PCR) in SCs, control cells transfected with a plasmid encoding a scramble shRNA (siScramble), and in cells transfected with a plasmid encoding a *Txnip* shRNA to knock down TXNIP expression (siTXNIP). In the absence of stimulation, silencing of TXNIP appears less effective when compared with siScramble cells than when compared with SCs. However, we observed a rapid induction of TXNIP expression after 2 hours of S100B treatment both in siScramble and SCs (Fig. 1A,B). Addition of an anti-RAGE blocking antibody (Perrone et al., 2009; Perrone et al., 2008) abolishes S100B-induced TXNIP expression (Fig. 1A,B). Src kinase mediates activation of RAGE downstream targets (Perrone et al., 2008; Reddy et al., 2006). The Src-specific inhibitor PP1 completely blocked S100B-induced TXNIP expression in siScramble and SCs (Fig. 1A,B). Silencing of TXNIP (Perrone et al., 2009) affected TXNIP expression in each condition analyzed (Fig. 1A,B). Stimulation with S100B for 2 hours in siScramble cells resulted in enhanced TXNIP protein levels that were abolished by either PP1 or an anti-RAGE blocking antibody, as well as by silencing of TXNIP (siTXNIP) (Fig. 1C,D). TXNIP protein expression in SC is still elevated following 24 hours of stimulation with S100B and is abolished in siTXNIP cells (Fig. 1E,F). For the first time, we show that TXNIP expression is enhanced in vivo during peripheral nerve injury. Partial rat sciatic nerve (SCN) ligature (Maeda et al., 2008) resulted in enhanced TXNIP protein expression from day 1 to day 6 following surgery (Fig. 2A,B). TXNIP protein level declined after 15 days following PLS and was comparable to the controls. No changes were observed in sham-operated SCN, which did not receive ligature (Fig. 2A,B). TXNIP expression in sham-operated SCN did not change relative to control unoperated SCN (not shown). These data further support our hypothesis about the role of TXNIP during peripheral nerve injury.

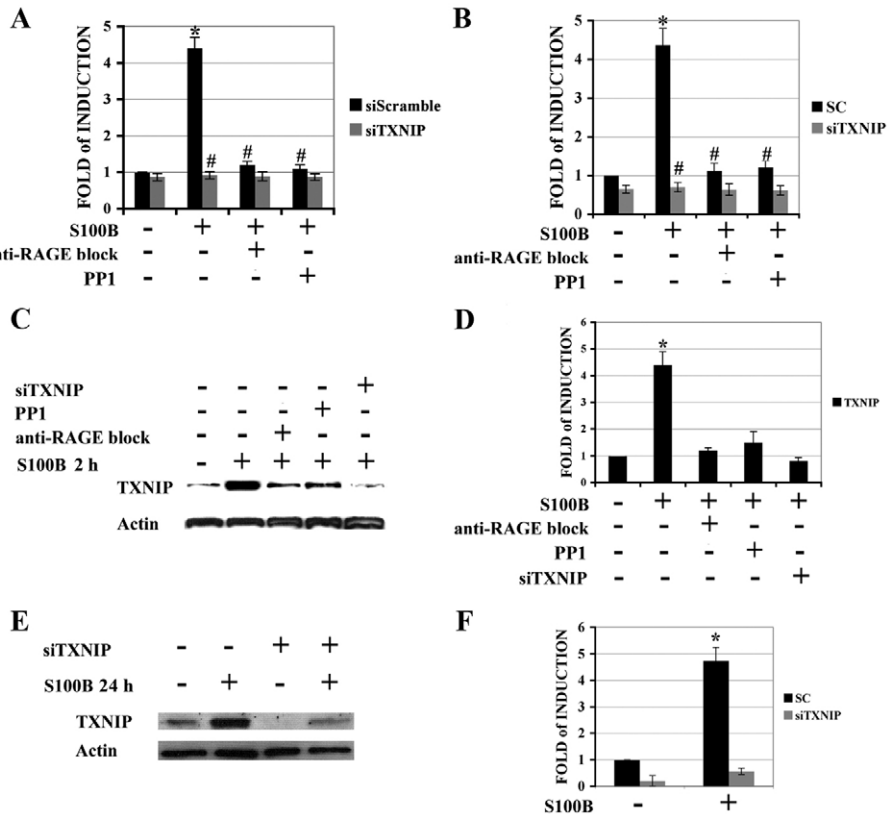


**Fig. 1. RAGE induces TXNIP expression in SCs.** siScramble (**A**), SC (**B**) and siTXNIP (A,B) were stimulated with S100B (10 µg/ml) for 2 hours and treated as indicated. *Txnip* mRNA expression was analyzed by qRT-PCR using actin as control gene for normalization. The results shown are the mean ± s.e. of three independent experiments carried out in triplicate ($n$=9). *$P$<0.001 versus control siScramble or SCs; $^{\#}P$<0.001 versus siScramble or SCs treated with S100B. (**C**–**F**) Western blot analysis of TXNIP and control actin expression ($n$=3). siScramble (C,D), SC (E,F) and siTXNIP (C–F) were stimulated with S100B (10 µg/ml) for 2 hours (C,D) or 24 hours (E,F) and treated as indicated. *$P$<0.001 indicates significant induction versus unstimulated cells.

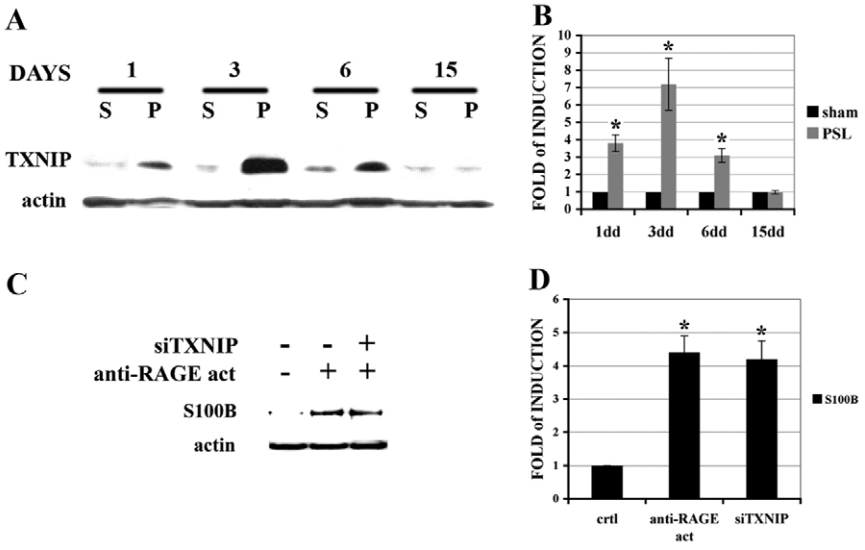


**Fig. 2. TXNIP expression is induced during peripheral nerve injury.** (**A**,**B**) Western blot analysis of TXNIP and actin expression in SCN following either PSL or sham operation. **P*<0.05 versus sham-operated (*n*=4). (**C**,**D**) siScramble and siTXNIP were incubated for 2 hours with an activating anti-RAGE antibody. The presence of S100B in the medium was evaluated by western blot. Actin was detected as a loading control. **P*<0.05 versus control siScramble (*n*=3).

Because we demonstrated that internalized RAGE colocalizes with endogenous S100B and induces S100B secretion in SC (Perrone et al., 2008), we analyzed whether TXNIP silencing affects RAGE-induced S100B secretion. Treatment with an anti-RAGE antibody that induces RAGE internalization (Perrone et al., 2008) promoted S100B secretion in siScramble as well as in siTXNIP cells (Fig. 2C,D). Thus, TXNIP is not involved in S100B secretion.

### Lipid rafts are involved in RAGE-induced S100B secretion in SCs

We demonstrated that RAGE induces cav-1 phosphorylation and colocalizes with phosphorylated cav-1 in an endocytic compartment (Perrone et al., 2008). We further investigated whether RAGE is internalized via lipid rafts and interacts with cav-1 in SCs. We stimulated RAGE with its ligand S100B for various times (Perrone et al., 2009; Perrone et al., 2008) and analyzed RAGE internalization using an endocytosis assay with a cleavable biotin (Perrone et al., 2005), to biotin-label RAGE at the cell surface and discriminate RAGE internalized in endocytic vesicle from cell surface RAGE (Perrone et al., 2008). We next isolated lipid-raft-associated RAGE by extraction in Triton X-100 at 4°C and pull down with neutravidin beads. In the absence of stimulation, biotinylated RAGE is exclusively associated to the Triton-insoluble fraction, which corresponds to lipid rafts as shown by the enrichment in cav-1 co-fractionation (Fig. 3A, time 0). RAGE is associated with lipid rafts almost completely following 5 and 20 minutes of stimulation with S100B (Fig. 3A). Also, non-biotinylated RAGE (total amount) is mostly associated with lipid rafts (Fig. 3A), suggesting that RAGE is also associated with lipid rafts during its targeting from the endoplasmic reticulum to the cell surface. We did not investigate this hypothesis because it is outside the scope of the present study. It is possible to argue that RAGE is present in the insoluble fraction because it is associated with the cytoskeleton. However, disruption of lipid rafts by cholesterol extraction with beta-cyclodestrin (β-CD) completely shifted RAGE to the soluble fraction (supplementary material Fig. S1A) and affects the endocytic targeting of RAGE (data not shown). RAGE co-immunoprecipitated with cav-1 in the absence of S100B and following stimulation with S100B (Fig. 3B).

SCs express endogenous S100B (Perrone et al., 2008). We discovered that internalized RAGE is targeted to S100B-positive vesicles, promoting S100B secretion in SCs (Donato et al., 2009; Leclerc et al., 2009; Perrone et al., 2008). We next investigated whether RAGE induces the recruitment of S100B in cav-1 positive vesicles following stimulation with an anti-RAGE antibody that promotes RAGE endocytosis (Perrone et al., 2008). In the absence of stimulation both S100B and cav-1 showed a diffuse staining rather than a defined colocalization in any specific compartment (Fig. 3C). Indeed, S100B is cytoplasmatic and is recruited in vesicles only after specific stimulation (Donato et al., 2009; Perrone et al., 2008). Five minutes after RAGE stimulation, S100B colocalized with cav-1 in vesicle-like structures and at the plasma membrane (Fig. 3C). We did not analyze RAGE endocytic trafficking and S100B secretion in SCs lacking cav-1 because we have already demonstrated that Src kinase-induced cav-1 phosphorylation regulates both events (Perrone et al., 2008). Perturbation of lipid raft organization by cholesterol depletion with β-CD completely inhibited RAGE-induced S100B secretion (Fig. 3D,E). These data further confirm the role of lipid rafts and cav-1 in RAGE function and S100B secretion.

### TXNIP is required for RAGE-induced p38 MAPK activation in SCs

RAGE induces p38 MAPK activation in smooth muscle cells (Reddy et al., 2006). In siScramble cells, 10 minutes of stimulation with S100B induced p38 MAPK activation, which was inhibited by either an anti-RAGE blocking antibody or PP1 (Fig. 4A,B). TXNIP enhances p38 MAPK activation by trapping Trx, which inhibits the ASK1 (apoptosis signal kinase 1)–p38 pathway (Chen et al., 2008; Perrone et al., 2009; Yamawaki et al., 2005). Silencing of TXNIP (siTXNIP) abolished RAGE-induced p38 MAPK phosphorylation (Fig. 4A,B). RAGE stimulation with S100B led to Src-dependent Erk1/2 activation in smooth muscle cells (Reddy et al., 2006). We observed induction of Erk1/2 phosphorylation after 10 minutes of S100B stimulation in siScramble, which was inhibited by either an anti-RAGE blocking antibody or PP1 (Fig. 4C,D). TXNIP silencing only moderately affected RAGE-induced Erk1/2 activation and their phosphorylation was also elevated after S100B addition to siTXNIP (Fig. 4C,D).

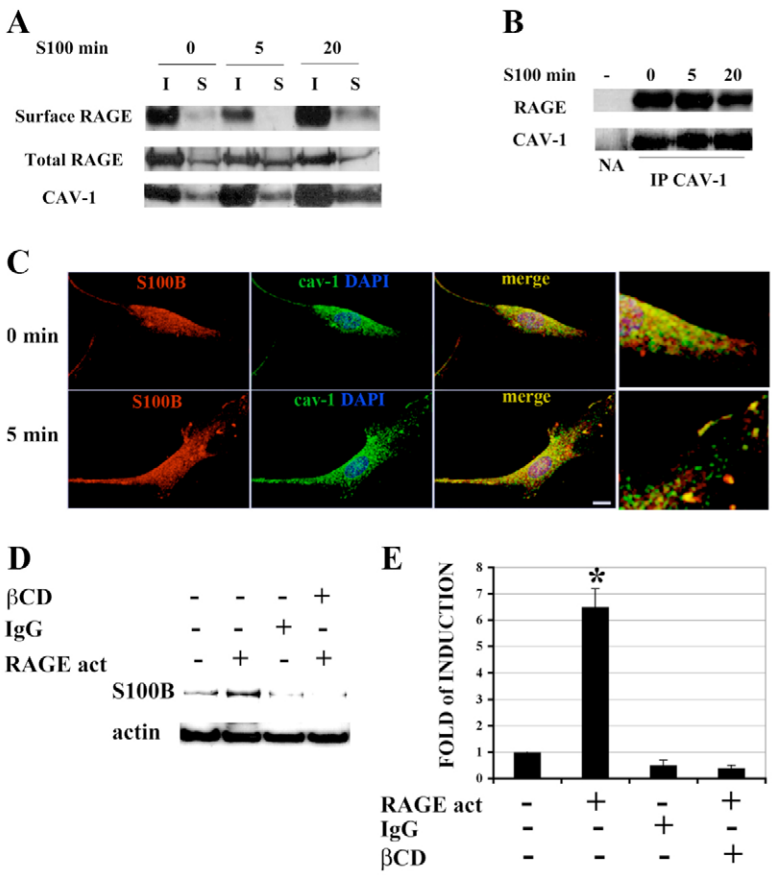


**Fig. 3. Lipid rafts are involved in RAGE-induced S100B secretion in SCs.** (**A**) SCs were surface biotinylated with NHS-SS–biotin and then incubated at 37°C with S100B (10 µg/ml). Surface biotin was cleaved by glutathione treatment at 4°C, whereas in internalized receptor, biotin was protected by the cleavage. Cells were lysed with 1% Triton X-100 at 4°C and both soluble and insoluble fraction were pulled down with Neutravidin beads. Biotinylated and total RAGE were detected by western blotting. (**B**) SCs were incubated at 37°C with S100B for the indicated times; immunoprecipitates with an anti-cav-1 antibody or a control IgG (NA) were subjected to western blot analysis as indicated. (**C**) Antibody-mediated RAGE internalization was carried out for the indicated time. The localization of S100B (red) and cav-1 (green) was analyzed by immunofluorescence and confocal microscopy. Magnification of the merge images is shown on the right to display the colocalization of S100B and cav-1 in vesicles and at the plasma membrane. A representative example of three independent experiments is shown. (**D**,**E**) SCs were incubated for 90 minutes with an anti-RAGE antibody that induces RAGE internalization or with a control IgG. Depletion of cholesterol was induced by treating SCs with β-CD (10 mM) 1 hour before the anti-RAGE addition. The medium was collected and precipitated using TCA. The presence of S100B was evaluated by western blotting. The amount of actin was analyzed as a control of the number of cells. Quantification of three independent experiments is shown in E. **P*<0.05 versus the control.

S100B induces cell migration in various cell types (Donato et al., 2009), but there are no reports on its effect on SC migration. We analyzed SC migration using Boyden chambers coated with FN because FN expression increases in nerve regeneration and correlates with SC migration and terminal differentiation (Akassoglou et al., 2002; Chernousov and Carey, 2000; Milner et al., 1997). S100B enhanced siScramble migration and this was inhibited by an anti-RAGE blocking antibody (Fig. 4E). The migration of siScramble was partially affected by the p38-specific inhibitor SB202190 and was completely blocked by the combined addition of SB202190 and PD98059; the latter inhibited MEK kinase, which is the upstream activator of Erk1/2 (Fig. 4E). These data are in agreement with the reported role of p38 MAPK and Erk1/2 on a SC cell line migration in vitro (Chang et al., 2009). Silencing of TXNIP affected S100B-enhanced SC migration only partially (Fig. 4E). Silencing of TXNIP also only partially affected SC migration in wound healing experiments (supplementary material Fig. S1B).

### TXNIP mediates RAGE-induced FN and Il-1β expression in SCs

SCs express FN following nerve injury (Akassoglou et al., 2002). S100B stimulation for 6 hours significantly enhanced *Fn* mRNA expression in siScramble compared with the control cells (Fig. 5A). Activation of p38 MAPK in SCs is required during the repair of the injured nerve (Haines et al., 2008). In agreement, the p38 MAPK inhibitor SB202190 completely abolishes S100B-induced FN expression (Fig. 5A). TXNIP induces nuclear translocation of NFκB (Aitken et al., 2004; Perrone et al., 2009). We prepared nuclear extracts as previously described (Perrone et al., 1999) and we verified by western blot analysis that RAGE activation by S100B leads to TXNIP-dependent nuclear translocation of NFκB (Fig. 5C,D). Blockade of NFκB nuclear translocation with a NFκB inhibitory peptide decreased FN expression significantly, but FN expression was still partially induced by S100B in siScramble cells (Fig. 5A). Silencing of TXNIP completely abolished FN expression following stimulation with S100B (Fig. 5A). We reported that phosphorylated cyclic AMP response element-binding protein (CREB), a major transcriptional co-activator in stress-signaling cascades, is involved in induction of FN expression in mesangial cells (Singh et al., 2003; Singh et al., 2001). Moreover, RAGE (Huttunen et al., 2002; Makam et al., 2009) and p38 MAPK (Ono and Han, 2000) induce CREB phosphorylation. Therefore, we investigated whether S100B promotes CREB phosphorylation via a RAGE–TXNIP pathway. In siScramble, S100B induced CREB phosphorylation that was inhibited by an anti-RAGE blocking antibody and by the p38 MAPK inhibitor SB202190 (Fig. 5E,F). In siTXNIP, S100B failed to promote CREB phosphorylation (Fig. 4E,F), showing that TXNIP is required for S100B-induced *Fn* mRNA expression by activating NFκB and CREB.

RAGE promotes expression of IL-1β in human monocytic THP-1 cells (Yeh et al., 2001) and in the RN-22 SC cell line in vitro (Sousa et al., 2001). S100B stimulation for 6 hours increased IL-1β mRNA (*Il1b*) expression of significantly in siScramble compared with the control untreated cells (Fig. 5B). An anti-RAGE blocking antibody, SB202190, as well as a NFκB inhibitory peptide completely abolished S100B-induced *Il1b* mRNA expression in siScramble cells (Fig. 5B) and silencing of TXNIP (siTXNIP) blocked IL-1β expression following S100B stimulation (Fig. 5B). We also investigated the protein level of immature IL-1β by western blotting and we observed the same results as those obtained by

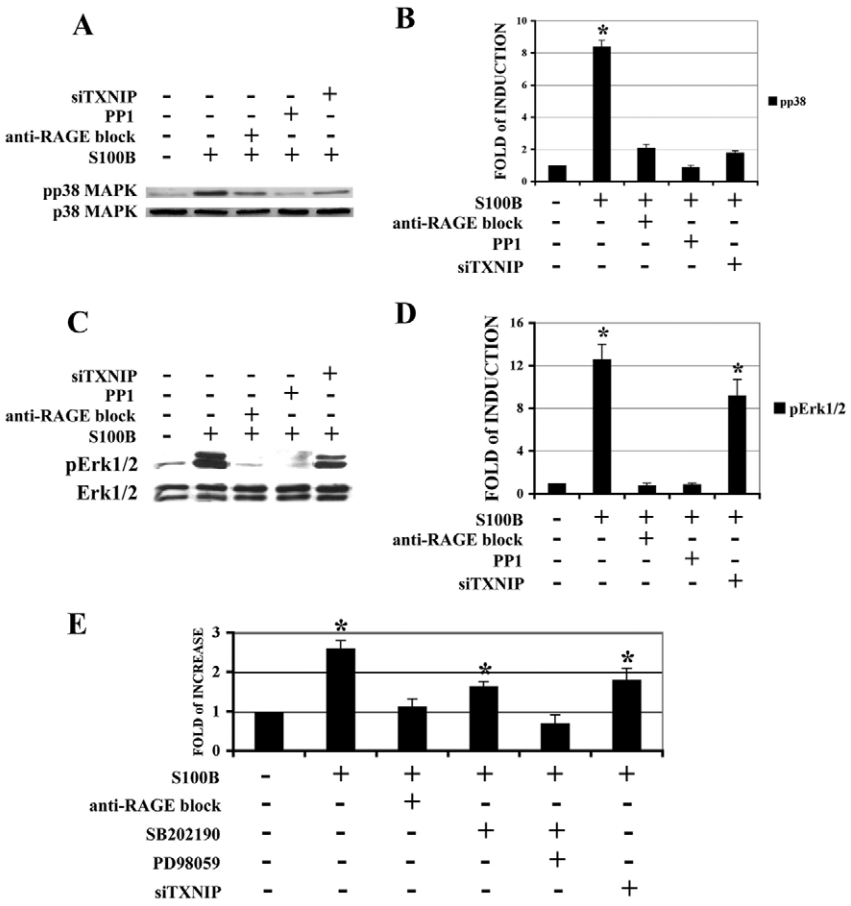


**Fig. 4. TXNIP is required for RAGE-induced p38 MAPK activation in SCs.** (**A–D**) siScramble and siTXNIP cells were stimulated with S100B (10 μg/ml) for 10 minutes and treated as indicated. Western blot analysis of total and phosphorylated p38 MAPK (A,B) and phosphorylated and total Erk1/2 (C,D). (**E**) Migration assay in Transwell chambers coated with FN (5 μg/ml). S100B was added in the bottom chamber. Cells were allowed to migrate for 6 hours and number of cells that migrated to the bottom side was counted. **P*<0.05 versus control siScramble (*n*=3).

qRT-PCR analysis of mRNA expression (Fig. 5G,H). We investigated using ELISA, whether S100B induces IL-1β secretion in the SC medium (Yeh et al., 2001). We observed a modest secretion of IL-1β in siScramble cells treated for 6 hours with S100B (supplementary material Table S1). Secretion of IL-1β was abolished with an anti-RAGE blocking antibody, SB202190, the NFκB inhibitory peptide, as well as by TXNIP silencing (supplementary material Table S1).

## Discussion

Several studies demonstrate that RAGE and its ligands exacerbate injury and participate in chronic disorders when they are chronically overexpressed. However, RAGE and its ligands participate in repair when their expression is transient following stress or injury (Rong et al., 2005). Indeed, RAGE and its ligand S100B are required for the repair of the injured sciatic nerve (Rong et al., 2004a). Since we found that TXNIP mediates RAGE-induced inflammation in retinal endothelial cells (Perrone et al., 2009), it was logical to determine whether the RAGE–TXNIP pathway is involved in the repair of the injured peripheral nerve. We hypothesized that a transient expression of TXNIP is beneficial in orchestrating the limited inflammatory mechanisms required for the repair of the injured peripheral nerve. In agreement with our hypothesis, we show here that TXNIP expression is strongly enhanced in vivo after sciatic nerve injury and that its overexpression is transient and is downregulated 15 days following injury.

Rapid reprogramming of SCs after peripheral nerve injury is necessary for the repair: SCs acquire mononuclear phagocytic-like properties and secrete provisional ECM required for their migration. Since it has been shown that SCs overexpress RAGE following sciatic nerve injury and S100B is required for the repair of the nerve (Rong et al., 2004a), we investigated whether the RAGE–TXNIP axis mediates SC functions following stimulation with S100B. We also dissected the signalling pathway induced by S100B–RAGE interaction. In agreement with previous reports (Perrone et al., 2008; Reddy et al., 2006), we found that Src activation is required for RAGE-induced TXNIP expression and RAGE-mediated signalling cascade.

TXNIP has no effect on RAGE-induced endogenous S100B secretion in SCs. On the contrary, we found that S100B secretion involves lipid rafts. In agreement, S100A8 and S100A9 are translocated to lipid rafts only upon calcium activation in neutrophils (Nacken et al., 2004). Although previous studies demonstrated that RAGE co-fractionates with cav-1 in endothelial cells (Lisanti et al., 1994) and colocalizes with cav-1 in smooth muscle cells (Reddy et al., 2006), we show that RAGE is internalized via lipid rafts and is present in a protein complex together with cav-1 (Perrone et al., 2008; Reddy et al., 2006).

p38 MAPK has a key role during myelination when it controls the differentiation of SCs (Haines et al., 2008). We found that TXNIP is required for RAGE-induced p38 MAPK activation and the subsequent events that are regulated by this signalling cascade. TXNIP only partially participates in RAGE-induced SC migration. SC migration depends on the activation of both p38 MAPK and MEK pathways (Chang et al., 2009). TXNIP ablation had no effect on RAGE-induced Erk1/2 activation, suggesting that TXNIP mediates RAGE-induced SC migration in part by modulating p38 MAPK activation.

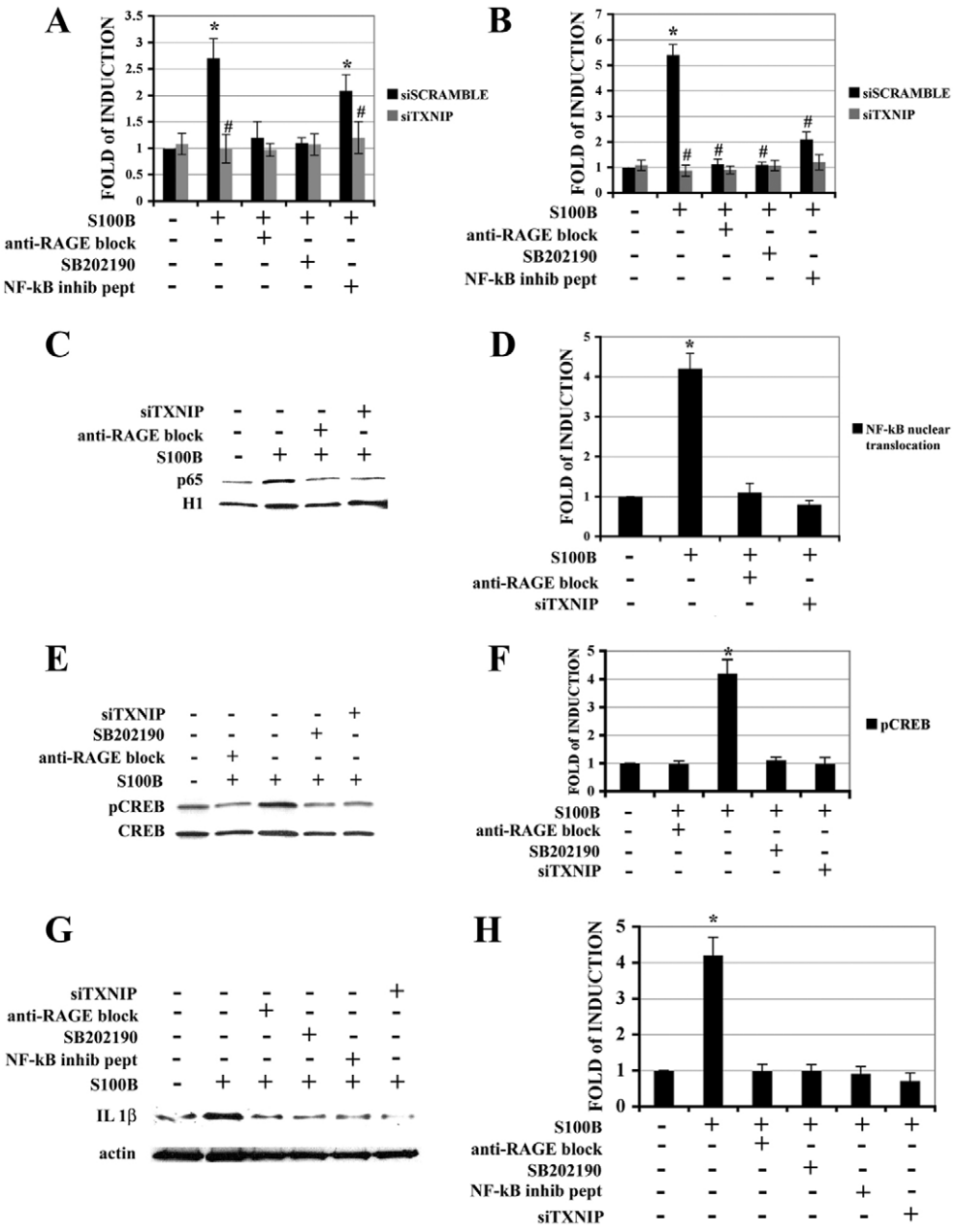


**Fig. 5. TXNIP mediates RAGE-induced FN and IL-1β expression in SCs.** siScramble and siTXNIP cells were stimulated with S100B (10 µg/ml) for 6 hours and treated as indicated. FN (**A**) and IL-1β (**B**) expression was analyzed by qRT-PCR using actin as control gene for normalization. These results are the mean ± s.e. of three independent experiments carried out in triplicate ($n$=9). *$P$<0.001 versus control siScramble; $^{\#}P$<0.001 versus siScramble treated with S100B. (**C**,**D**) The presence of the p65 subunit of NFκB in the nuclear extracts analyzed by western blotting. The total amount of protein load was normalized by western blotting analysis of the histone H1. Western blot analysis of phosphorylated and total CREB (**E**,**F**) and of IL-1β and control actin (**G**,**H**). *$P$<0.001 versus control siScramble ($n$=3).

In agreement, with the role of TXNIP in the RAGE-induced p38 MAPK cascade, we found that TXNIP is required for FN expression by inducing NFκB nuclear translocation and CREB phosphorylation.

SCs produces the pro-inflammatory cytokine IL-1β in vivo following axonal injury and it has been suggested that IL-1β protects SCs and aids in the repair process (Lisak et al., 1997; Shamash et al., 2002). Indeed, we found that TXNIP is necessary for RAGE-induced Il-1β expression and secretion. A recent study demonstrates that TXNIP induces the secretion of IL-1β by activating the NLRP3 inflammasome in macrophages exposed to oxidative stress, leading to caspase-1 activation and production of the mature form of IL-1β (Zhou et al., 2010). Macrophages express a constitutive high protein level of TXNIP, which dissociates from thioredoxin in the presence of oxidative stress and activates NLRP3. On the contrary, SCs do not show a constitutively high expression of TXNIP, and RAGE does not induce detectable oxidative stress in SCs (data not shown). Our data strongly indicate that the modest secretion of IL-1β by SCs following S100B stimulation is mostly a consequence of RAGE-induced *Il1b* mRNA expression. Indeed, it is inhibited by the NFκB inhibitory peptide. In agreement with our hypothesis, a similar regulation has been shown in THP-1 cells (Yeh et al., 2001). We speculate that the modest IL-1β secretion induced by RAGE in SCs could be beneficial and enhance the repair of the injured nerve. In agreement, SCs express and secrete IL-1β following sciatic nerve crush injury in vivo and IL-1β promotes neurite outgrowth in cultured dorsal root ganglia (DRG) in vitro (Temporin et al., 2008).

In conclusion, the present study reveals that RAGE induces TXNIP expression in SCs. TXNIP is partly involved in RAGE-induced SC migration and is required for RAGE-induced FN and IL-1β expression by activating p38 MAPK, CREB and NFκB. Our

results support a model in which TXNIP mediates in part RAGE-induced SC migration and is required for the expression of provisional ECM and pro-inflammatory IL-1β, shedding new light on the role of RAGE and S100B in the repair of the injured peripheral nerve. In agreement, we show that TXNIP expression is induced by SCN injury and its expression declines to control levels 15 days following damage.

## Materials and Methods

### Material

Anti-TXNIP (MBL Biotechnology, Beaver, MA); anti-actin and anti-p65 NFκB subunit, anti phosphorylated p38 MAPK, anti-p38 MAPK, anti-phosphorylated and total Erk1/2, anti phosphorylated and total CREB (Cell Signaling Solutions, Lake Placid, NY); anti-histone H1, anti-IL-1β (Abcam, Cambridge, MA); anti-RAGE blocking antibody (R&D System, Minneapolis, MN); anti-RAGE (H300) (Santa Cruz Biotechnology, CA); anti-S100B (Chemicon, Millipore, Millerica, MA); anti-cav-1 (BD-Bioscience) antibodies were sourced. FITC and TRITC secondary antibodies were from Molecular Probes (Invitrogen, Carlsbad, CA). The enhanced chemiluminescence (ECL) system was from Amersham (Arlington Heights, IL). DMEM and F-12 nutrient mixture (Ham's) were from GIBCO (Grand Island, NY). S100B protein was purchased from Calbiochem (EMD, San Diego, CA). SN50 cell-permeable NFκB Inhibitor Peptide, SB202190, PD98059, and PP1 (pyrazolo pyrimidine-type inhibitor 1) were also from Calbiochem (San Diego, CA). Enzyme-linked immunosorbent assay (ELISA) for IL-1β was from (R&D System, Minneapolis, MN). HRP-linked streptavidin and streptavidin–agarose beads were from Pierce.

### SC culture

Rat SC primary cultures were obtained, cultured, and treated as previously described (Perrone et al., 2008; Perrone et al., 2009). 1 day before stimulation with S100B, SCs were serum starved in SCDM medium (Perrone et al., 2008). PP1 (5 μM) was added 45 minutes before and during S100B stimulation. SB202190 (10 μM) and PD98059 (50 μM) were added 30 minutes before and during S100B stimulation. Cell-permeable NFκB inhibitory peptide (50 μg/ml) were added 30 minutes before and during S100B stimulation.

### Generation of stably transfectant SCs

We obtained siScramble and siTXNIP cells (Perrone et al., 2009) as previously reported. Briefly, to knock down TXNIP expression, we stably transfected the cells with a plasmid carrying a double-stranded oligonucleotide targeted to the rat *Txnip* mRNA (Super Array Bioscience Corporation, Frederick, MD), as recently described (Perrone et al., 2009). As a control, a plasmid encoding a scramble RNA was transfected. These plasmids also carry the selection marker that confers resistance to neomycin. We isolated resistant transfected cells. Silencing of TXNIP expression was analyzed by real-time quantitative PCR and western blot analysis.

### Endocytosis assay

We performed endocytosis assay as previously described (Perrone et al., 2005; Perrone et al., 2008). Briefly, cells were biotinylated using cleavable biotin: sulphosuccinimidyl-6-(biotinamide) hexanoate (NHS-SS-biotin) as previously described (Perrone et al., 2008). Samples were incubated at 37°C for different times in the presence of S100B, whereas control filters were kept at 4°C. After incubation, cells were lysed in RIPA buffer (10 mM Tris-HCl, pH 8, 1% Triton X-100, 0.1% DOC, 0.1% SDS, 140 mM NaCl and 1 mM PMSF). Biotinylated antigens were pulled down with streptavidin–agarose beads. After beads were boiled in Laemmli buffer, supernatants were analyzed by SDS-PAGE and fluorography with pre-flashed films. To control the total amount of RAGE, 1/10th of the supernatant was analyzed by western blotting.

### Western blotting

Preparation of total and nuclear extracts and western blots (Perrone et al., 2009; Perrone et al., 1999; Vincent et al., 2007) were performed as previously described.

### Triton X-100 extraction of lipid-raft-associated proteins

Cells were lysed at 4°C in Triton X-100 and the soluble and insoluble fractions were obtained as previously reported (Paladino et al., 2007).

### Antibody-mediated internalization assay

Antibody-mediated internalization is a technique that has been extensively applied to investigate the endocytic fate of various receptors and membrane-associated proteins (Millan et al., 2006; Perrone et al., 2008; Tampellini et al., 2007). SCs were starved in SCDM for 24 hours. Rabbit anti-RAGE antibody (1 mg/ml) (H-300, Santa Cruz Biotechnology, Santa Cruz, CA) was added for 30 minutes at 4°C in incubation medium (DMEM, 10 mM HEPES pH 7.5, 0.2% BSA). The specificity of this antibody has been previously verified and it has been used to detect RAGE subcellular localization in vesicles by colocalization experiments and immunofluorescence analysis (Hermani et al., 2006).

### Immunofluorescence analysis

We performed immunofluorescence analysis as previously described (Perrone et al., 2008). Briefly, we induced RAGE internalization by antibody-mediated internalization assay. SCs were fixed in 4% PFA in PBS containing 1.8 mM $Ca^{2+}$ and 0.5 mM $Mg^{2+}$ (PBS/CM). SC were permeabilized in PBS/CM containing 0.15% Triton X-100 for 5 minutes, blocked with PBS/CM containing 0.05% Triton X-100 and 1% BSA for 30 minutes. Cells were incubated for 1 hour at room temperature (RT) with the appropriated primary antibody, washed with PBS/CM and treated for 1 hour at RT with the appropriate secondary antibody.

Analysis of immunofluorescence was performed with an Olympus FluoView 500 laser scanning confocal microscope. Samples were visualized with an Olympus IX-71 inverted microscope using a 60× oil-immersion lens, magnified twice with FluoView version 5.0 software and scanned sequentially to maximize signal separation. DAPI, Alexa Fluor 488 and Alexa Fluor 594 fluorescence was excited with a 405 nm blue laser diode, 488 nm argon blue and 543 nm helium neon laser, respectively. Emissions were separated with 430–460 nm, 505–525 nm and 610 nm barrier filters.

### Immunoprecipitation and immunoblot analysis

Cells were washed twice with ice-cold PBS/CM and lysed as described elsewhere (Perrone et al., 2008). Samples were immunoprecipitated with the following antibodies: rabbit anti-cav-1, 1:100 (N-20, Santa Cruz Biotechnology), rabbit polyclonal anti-RAGE, 1:100 (H-300, Santa Cruz Biotechnology). Western blot analysis was carried out with the following antibodies: mouse anti-rabbit anti-cav-1, 1:1000 (BD Transduction, cat. no. 610406), mouse anti-RAGE 1:500 (RD Systems, cat. no. MAB1179). For analysis of S100B secretion, SC medium was precipitated with TCA. Western blot analysis was carried out with mouse anti-S100B (Chemicon, cat. no. MAB079-1).

### Reverse-transcription quantitative PCR (qRT-PCR)

mRNA expression was analyzed by qRT-PCR using the BioRad Chromo 4 detection system and SYBR Green PCR Master Mix from Applied Biosystems (Foster City, CA) as previously described (Cheng et al., 2006; Perrone et al., 2009). Primers were synthesized by Invitrogen (Carlsbad, CA). Cycle threshold (*Ct*) values were used to calculate the relative expression level of the various mRNAs that were normalized to actin mRNA. Primers for fibronectin and actin are for mouse and also recognize the rat genes. As negative controls, the same reaction was performed on RNA samples without the reverse transcriptase reaction, and no PCR products were detected. QRT-PCR primers are indicated in supplementary material Table S2.

### SC migration

Migration of Schwann cells was studied using 6.5 mm Transwell chambers with 8 μm pores (Corning Costar, Corning, NY). The bottom surface of each membrane was coated with FN (5 μg/ml). SCs (100,000) in SDCM were allowed to adhere for 1 hour. S100B was added to the bottom chamber. Cells were allowed to migrate for 6 hours at 37°C. The upper surface of each membrane was cleaned with a cotton swab. The membranes then were stained with DAPI. The number of cells on the bottom surface of each membrane was counted.

### Wound healing

Cells were seeded uniformly on FN coated coverslips. We created an artificial 'wound' at 0 hours, using a sterile P-200 pipette tip to scratch the sub-confluent cell monolayer. Cell migration was analyzed after 6 hours of culture. Photographs were taken of the wounded regions using an inverted Olympus microscope.

### Measurement of IL-1β secretion

ELISA was used for the quantitative measurement of released IL-1β. After treatment of the cells, the media was collected and analyzed by ELISA according to the protocol provided by the manufacturer (R&D System).

### Partial sciatic nerve ligature (PLS)

All procedures were performed according to the French law on Animal Care Guidelines. Animal Care Committee of UniversityAix-Marseille II approved protocols. Male Sprague-Dawley rats were subjected to PLS according to Maeda et al protocol (Maeda et al., 2008). Briefly, rats were anesthetized with pentobarbital (80 mg/kg). The sciatic nerve (SCN) of right lateral hindlimb was exposed just below the hipbone, and half of the sciatic nerve was tightly ligated with silk suture thread (PSL). As control treatment, called sham, the SCN of left lateral hindlimb of the same rat was exposed, but was not subjected to ligation. The sham-operated of the left hindlimb was used as control for each right lateral PSL in western blot analysis of TXNIP protein expression. For each point of the time course, four different rats were analyzed ($n$=4): right sciatic nerve for PSL and the left sciatic nerve of the same animal as sham-operated control. Moreover, four rats not-operated neither on the right nor on the left hindlimb were used to investigate TXNIP expression in comparison to sham-operated left hindlimb. There is not difference in

TXNIP protein level between these controls and sham-operated left hindlimb (data not shown).

This study was supported by the Marie Curie International Reintegration Grant from European Community (number 224892) to L.P. and by WSU School of Medicine, Detroit, to L.P.S. This article is freely accessible online from the date of publication.

Supplementary material available online at
http://jcs.biologists.org/cgi/content/full/123/24/4332/DC1

## References


**Aitken, C., Hodge, J., Nishinaka, Y., Vaughan, T., Yodoi, J., Day, C., Morrison, N. and Nicholson, G.** (2004). Regulation of human osteoclast differentiation by thioredoxin binding protein-2 and redox-sensitive signaling. *J. Bone Miner. Res.* **19**, 2057-2064.

**Akassoglou, K., Yu, W. M., Akpinar, P. and Strickland, S.** (2002). Fibrin inhibits peripheral nerve remyelination by regulating Schwann cell differentiation. *Neuron* **33**, 861-875.

**Bierhaus, A., Humpert, P. M., Morcos, M., Wendt, T., Chavakis, T., Arnold, B., Stern, D. M. and Nawroth, P. P.** (2005). Understanding RAGE, the receptor for advanced glycation end products. *J. Mol. Med.* **83**, 876-886.

**Chang, Y. M., Shih, Y. T., Chen, Y. S., Liu, C. L., Fang, W. K., Tsai, C. H., Tsai, F. J., Kuo, W. W., Lai, T. Y. and Huang, C. Y.** (2009). Schwann cell migration induced by earthworm extract via activation of PAs and MMP2/9 mediated through ERK1/2 and p38. *Evid. Based Complement. Alternat. Med.* Epub ahead of print.

**Chen, C. L., Lin, C. F., Chang, W. T., Huang, W. C., Teng, C. F. and Lin, Y. S.** (2008). Ceramide induces p38 MAPK and JNK activation through a mechanism involving a thioredoxin-interacting protein-mediated pathway. *Blood* **111**, 4365-4374.

**Cheng, C. and Zochodne, D. W.** (2002). In vivo proliferation, migration and phenotypic changes of Schwann cells in the presence of myelinated fibers. *Neuroscience* **115**, 321-329.

**Cheng, D. W., Jiang, Y., Shalev, A., Kowluru, R., Crook, E. D. and Singh, L. P.** (2006). An analysis of high glucose and glucosamine-induced gene expression and oxidative stress in renal mesangial cells. *Arch. Physiol. Biochem.* **112**, 189-218.

**Chernousov, M. A. and Carey, D. J.** (2000). Schwann cell extracellular matrix molecules and their receptors. *Histol. Histopathol.* **15**, 593-601.

**Cohen, A. W., Hnasko, R., Schubert, W. and Lisanti, M. P.** (2004). Role of caveolae and caveolins in health and disease. *Physiol. Rev.* **84**, 1341-1379.

**Donato, R., Sorci, G., Riuzzi, F., Arcuri, C., Bianchi, R., Brozzi, F., Tubaro, C. and Giambanco, I.** (2009). S100B's double life: intracellular regulator and extracellular signal. *Biochim. Biophys. Acta* **1793**, 1008-1022.

**Haines, J. D., Fragoso, G., Hossain, S., Mushynski, W. E. and Almazan, G.** (2008). p38 Mitogen-activated protein kinase regulates myelination. *J. Mol. Neurosci.* **35**, 23-33.

**Hermani, A., De Servi, B., Medunjanin, S., Tessier, P. A. and Mayer, D.** (2006). S100A8 and S100A9 activate MAP kinase and NF-kappaB signaling pathways and trigger translocation of RAGE in human prostate cancer cells. *Exp. Cell Res.* **312**, 184-197.

**Huttunen, H. J., Kuja-Panula, J. and Rauvala, H.** (2002). Receptor for advanced glycation end products (RAGE) signaling induces CREB-dependent chromogranin expression during neuronal differentiation. *J. Biol. Chem.* **277**, 38635-38646.

**Kim, S. Y., Suh, H. W., Chung, J. W., Yoon, S. R. and Choi, I.** (2007). Diverse functions of VDUP1 in cell proliferation, differentiation, and diseases. *Cell. Mol. Immunol.* **4**, 345-351.

**Leclerc, E., Fritz, G., Vetter, S. W. and Heizmann, C. W.** (2009). Binding of S100 proteins to RAGE: an update. *Biochim Biophys Acta* **1793**, 993-1007.

**Lisak, R. P., Skundric, D., Bealmear, B. and Ragheb, S.** (1997). The role of cytokines in Schwann cell damage, protection, and repair. *J. Infect. Dis.* **176**, S173-S179.

**Lisanti, M. P., Scherer, P. E., Vidugiriene, J., Tang, Z., Hermanowski-Vosatka, A., Tu, Y. H., Cook, R. F. and Sargiacomo, M.** (1994). Characterization of caveolin-rich membrane domains isolated from an endothelial-rich source: implications for human disease. *J. Biol. Chem.* **126**, 111-126.

**Maeda, T., Kiguchi, N., Kobasaky, Y., Ozaki, M. and Kisshiota, S.** (2008). Pioglitazone attenuates tactile allodynia and thermal hyperalgesia in mice sbjeced to peripheral nerve injury. *J. Pharmacol. Sci*. **108**, 341-347.

**Makam, M., Diaz, D., Laval, J., Gernez, Y., Conrad, C. K., Dunn, C. E., Davies, Z. A., Moss, R. B., Herzenberg, L. A. and Tirouvanziam, R.** (2009). Activation of critical, host-induced, metabolic and stress pathways marks neutrophil entry into cystic fibrosis lungs. *Proc. Natl. Acad. Sci. USA* **106**, 5779-5783.

**Mikol, D. D., Scherer, S. S., Duckett, S. J., Hong, H. L. and Feldman, E. L.** (2002). Schwann cell caveolin-1 expression increases during myelination and decreases after axotomy. *Glia* **38**, 191-199.

**Millan, J., Hewlett, L., Glyn, M., Toomre, D., Clark, P. and Ridley, A. J.** (2006). Lymphocyte transcellular migration occurs through recruitment of endothelial ICAM-1 to caveola- and F-actin-rich domains. *Nat. Cell Biol.* **8**, 113-123.

**Milner, R., Wilby, M., Nishimura, S., Boylen, K., Edwards, G., Fawcett, J., Streuli, C., Pytela, R. and ffrench-Constant, C.** (1997). Division of labor of Schwann cell integrins during migration on peripheral nerve extracellular matrix ligands. *Dev. Biol.* **185**, 215-228.

**Nacken, W., Sorg, C. and Kerkhoff, C.** (2004). The myeloid expressed EF-hand proteins display a diverse pattern of lipid raft association. *FEBS Lett.* **572**, 289-293.

**Ono, K. and Han, J.** (2000). The p38 signal transduction pathway: activation and function. *Cell. Signal.* **12**, 1-13.

**Paladino, S., Sarnataro, D., Tivodar, S. and Zurzolo, C**. (2007). Oligomerization is a specific requirement for apical sorting of glycosyl-phosphatidylinositol-anchored proteins but not for non-raft-associated apical proteins. *Traffic* **8**, 251-258.

**Perrone, L. and Zurzolo, C.** (2003). Lipid rafts and host cell-pathogen interactions. In *Intracellular Pathogens in Membrane Interactions and Vacuole Biogenesis* (ed. L. Perrone and C. Zurzolo), pp. 34-50. Georgetown, TX: Landes Bioscience.

**Perrone, L., Tell, G. and Di Lauro, R.** (1999). Calreticulin enhances the transcriptional activity of thyroid transcription factor-1 by binding to its homeodomain. *J. Biol. Chem.* **274**, 4640-4645.

**Perrone, L., Paladino, S., Mazzone, M., Nitsch, L., Gulisano, M. and Zurzolo, C.** (2005). Functional interaction between p75NTR and TrkA: the endocytic trafficking of p75NTR is driven by TrkA and regulates TrkA-mediated signalling. *Biochem. J.* **385**, 233-241.

**Perrone, L., Peluso, G. and Melone, M. A.** (2008). RAGE recycles at the plasma membrane in S100B secretory vesicles and promotes Schwann cells morphological changes. *J. Cell. Physiol.* **217**, 60-71.

**Perrone, L., Devi, T. S., Hosoya, K. I., Terasaki, T. and Singh, L. P.** (2009). Thioredoxin interacting protein (TXNIP) induces inflammation through chromatin modification in retinal capillary endothelial cells under diabetic conditions. *J. Cell. Physiol.* **221**, 262-272.

**Reddy, M. A., Li, S., Sahar, S., Kim, Y. S., Xu, Z. G., Lanting, L. and Natarajan, R.** (2006). Key role of Src kinase in S100B-induced activation of the receptor for advanced glycation end products in vascular smooth muscle cells. *J. Biol. Chem.* **281**, 13685-13693.

**Rong, L. L., Trojaborg, W., Qu, W., Kostov, K., Yan, S. D., Gooch, C., Szabolcs, M., Hays, A. P. and Schmidt, A. M.** (2004a). Antagonism of RAGE suppresses peripheral nerve regeneration. *FASEB J.* **18**, 1812-1817.

**Rong, L. L., Yan, S. F., Wendt, T., Hans, D., Pachydaki, S., Bucciarelli, L. G., Adebayo, A., Qu, W., Lu, Y., Kostov, K. et al.** (2004b). RAGE modulates peripheral nerve regeneration via recruitment of both inflammatory and axonal outgrowth pathways. *FASEB J.* **18**, 1818-1825.

**Rong, L. L., Gooch, C., Szabolcs, M., Herold, K. C., Lalla, E., Hays, A. P., Yan, S. F., Shi Du Yan, S. and Schmidt, A. M.** (2005). RAGE: A journey from the complications of diabetes to disorders of the nervous system-striking a fine balance between injury and repair. *Restorative Neurology and Neurosci.* **23**, 355-365.

**Shamash, S., Reichert, F. and Rotshenker, S.** (2002). The cytokine network of Wallerian degeneration: tumor necrosis factor-alpha, interleukin-1alpha, and interleukin-1beta. *J. Neurosci.* **22**, 3052-3060.

**Shao, Y., Kim, S. Y., Shin, D., Kim, M. S., Suh, H. W., Piao, Z. H., Jeong, M., Lee, S. H., Yoon, S. R., Lim, B. H. et al.** (2010). TXNIP regulates germinal center generation by suppressing BCL-6 expression. *Immunol. Lett.* **129**, 78-84.

**Singh, L. P., Andy, J., Anyamale, V., Greene, K., Alexander, M. and Crook, E. D.** (2001). Hexosamine-induced fibronectin protein synthesis in mesangial cells is associated with increases in cAMP responsive element binding (CREB) phosphorylation and nuclear CREB: the involvement of protein kinases A and C. *Diabetes* **50**, 2355-2362.

**Singh, L. P., Alexander, M., Greene, K. and Crook, E. D.** (2003). Overexpression of the complementary DNA for human glutamine:fructose-6-phosphate amidotransferase in mesangial cells enhances glucose-induced fibronectin synthesis and transcription factor cyclic adenosine monophosphate-responsive element binding phosphorylation. *J. Investig. Med.* **51**, 32-41.

**Sousa, M. M., Du Yan, S., Fernandes, R., Guimaraes, A., Stern, D. and Saraiva, M. J.** (2001). Familial amyloid polyneuropathy: receptor for advanced glycation end products-dependent triggering of neuronal inflammatory and apoptotic pathways. *J. Neurosci.* **21**, 7576-7586.

**Tampellini, D., Magrané, J., Takahashi, R. H., Li, F., Lin, M. T., Almeida, C. G. and Gouras, G. K.** (2007). Internalized antibodies to the Abeta domain of APP reduce neuronal Abeta and protect against synaptic alterations. *J. Biol. Chem.* **282**, 18895-18906.

**Temporin, K., Tanaka, H., Kuroda, Y., Okada, K., Yachi, K., Moritomo, H., Murase, T. and Yoshikawa, H.** (2008). IL-1beta promotes neurite outgrowth by deactivating RhoA via p38 MAPK pathway. *Biochem. Biophys. Res. Commun.* **365**, 375-380.

**Vincent, A. M., Perrone, L., Sullivan, K. A., Backus, C., Sastry, A. M., Lastoskie, C. and Feldman, E. L.** (2007). Receptor for advanced glycation end products activation injures primary sensory neurons via oxidative stress. *Endocrinology* **148**, 548-558.

**Yamawaki, H., Pan, S., Lee, R. and Berk, B.** (2005). Fluid shear stress inhibits vascular inflammation by decreasing thioredoxin-interacting protein in endothelial cells. *J. Clin. Invest.* **115**, 733-738.

**Yeh, C. H., Sturgis, L., Haidacher, J., Zhang, X. N., Sherwood, S. J., Bjercke, R. J., Juhasz, O., Crow, M. T., Tilton, R. G. and Denner, L.** (2001). Requirement for p38 and p44/p42 mitogen-activated protein kinases in RAGE-mediated nuclear factor-kappaB transcriptional activation and cytokine secretion. *Diabetes* **50**, 1495-1504.

**Zhou, R., Tardivel, A., Thorens, B., Choi, I. and Tschopp, J.** (2010). Thioredoxin-interacting protein links oxidative stress to inflammasome activation. *Nat. Immunol.* **11**, 136-140.